Observations of Periodic Intensity Bursts during the Start-Up Phase of a Free-Electron-Laser Oscillator

E. Jerby,[a] G. Bekefi, and J. S. Wurtele

Department of Physics, Research Laboratory of Electronics and Plasma Fusion Center, Massachusetts Institute of Technology, Cambridge, Massachusetts 02139

(Received 11 April 1990)

Observations of periodic intensity bursts during the start-up phase of a free-electron-laser oscillator operating in the microwave regime are reported. The bursts are composed of radiation micropulses several nanoseconds wide and separated by the resonant-cavity round-trip time (~35 ns). The occurrence of the bursts is correlated to random current spikes superposed on the continuous electron-beam current density. The observations are compared with theoretical results from an impulse response model of a free-electron laser.

PACS numbers: 42.55.Tb, 42.60.Fc, 52.75.Ms, 85.10.Jz

The study of the frequency spectrum and temporal evolution of electromagnetic pulses in lasers is a subject of considerable interest. In conventional atomic and molecular lasers short-pulse phenomena have been known for many years. These include the nonlinear phenomenon of self (spontaneous) spiking[1] as well as a wide range of mode-locking mechanisms[2] and soliton formation.[3]

In free-electron-laser (FEL) oscillators, radiation bursts, or spikes, as they are often called, have been studied experimentally and theoretically in the nonlinear regime by several groups.[4-11] The appearance of bursts in this nonlinear FEL regime comes about as a result of the FEL sideband instability caused by electron oscillations in the potential wells of the ponderomotive wave.

In contrast, studies in this Letter[12] deal with the build-up of short electromagnetic radiation bursts well before saturation and near oscillation threshold, where linear phenomena dominate the interaction. Here an observed radiation burst consists of periodic micropulses contained within a bell-shaped macropulse envelope. The start-up of the radiation macropulses are correlated with random current spikes superposed on a uniform current-density beam. The experimental observations agree with a theoretical linear model of the FEL impulse response in the time domain. The results shed light on start-up processes, mode locking, and micropulse formation in FEL oscillators.

Figure 1(a) shows a schematic of our experiment.[13] The accelerating potential is supplied by a Marx generator (Physics International Pulserad 615 MR). The electron beam is generated by a thermionically emitting, electrostatically focused, Pierce-type electron gun (250 kV, 250 A) from a SLAC klystron (model 343). An emittance selector is used to limit the beam current to ~1 A. An assembly of focusing coils transports the electron beam into the rectangular stainless-steel drift tube (0.40″×0.90″), which also acts as the waveguide for the electromagnetic radiation. The beam is contained by a uniform 1.6-kG axial magnetic field produced by a solenoid.

A 65-period circularly polarized magnetic wiggler has a period $l_w = 3.5$ cm, an amplitude $B_w = 200$–400 G, and is generated by bifilar conductors.[13,14] Since an aperture

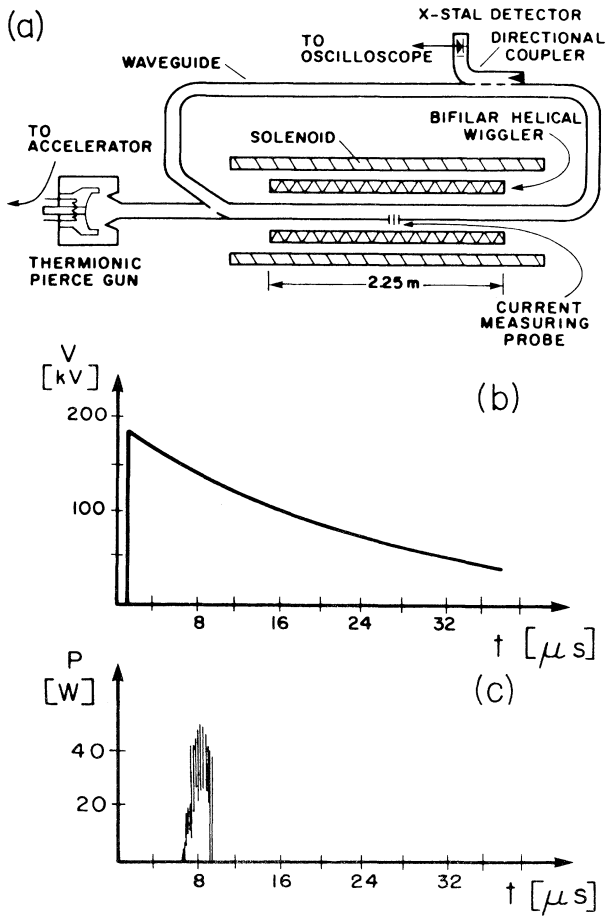

FIG. 1. (a) Experimental arrangement showing the ring cavity of the FEL oscillator; (b),(c) typical oscilloscope traces of the beam voltage and a radiation burst, respectively.

limits the size of the electron beam to $r_b \simeq 0.07 l_w$, the wiggler field appears nearly sinusoidal to the drifting electrons. At the wiggler entrance a slowly increasing field amplitude is produced by resistively loading the first six periods of the wiggler magnet.

The 2.7-m-long drift tube acts as a rectangular waveguide whose fundamental TE_{10} mode has a cutoff frequency of 6.6 GHz. The drift tube closes upon itself and thereby forms a ring cavity 7.6 m in length [see Fig. 1(a)]. The system is operated in a frequency range between 8 and 11 GHz. At those frequencies the empty waveguide can support only the fundamental (TE_{10}) mode, all higher modes being evanescent. The ring-cavity loss is 5.5 dB. The single-pass FEL gain varies between 6 and 8.5 dB, so that the overall system gain is less than 3 dB. It is in this low-net-gain operating regime that all of our measurements are carried out, and where the periodic rf spikes are the clearest. In order to observe the rf bursts, the radiation field of the ring cavity is sampled by means of a 20-dB directional coupler and a high-pass filter ($f > 9.6$ GHz), and then measured with a calibrated crystal detector.

Figures 1(b) and 1(c) illustrate the time history of the beam energy and the rf power as observed on an oscilloscope screen. Since our Marx accelerator has an RC droop with a 25-μs time constant, the electron-beam energy sweeps through the range of values illustrated in Fig. 1(b). Figure 1(c) shows that under these experimental conditions the overall rf bursts start ~ 7 μs after the Marx ignition and last typically for 1–2 μs.

The radiation bursts and the electron-beam current are recorded simultaneously by a fast two-channel digital oscilloscope (LeCroy 7200, with 1-GHz sampling rate). The stored numerical data enable a precise analysis of the rf intensity and the current fluctuations, and of the correlation between these signals. Figure 2(a) shows a typical example of the radiation bursts on an expanded scale. Two dominant macropulses, marked as A and B, are clearly seen within partially overlapping bell-shaped envelopes. Each macropulse consists of a series of micropulses; the distance between two successive micropulses is 32 ns in macropulse A, and 34 ns in B. The micropulse width in both macropulses is 5.3 ns, and no significant broadening is observed in successive round-trips near the macropulse peak.

In all the runs performed (over 100), the bell-shaped macropulse constitutes the basic building block of a radiation burst with random start-up times. The time between successive micropulses within each macropulse equals the round-trip time of the FEL radiation in the cavity, as determined by the cavity length and the instantaneous electron-beam energy.

Figure 2(b) shows the electron-beam current as a function of time as detected by a tiny probe[14] partially inserted within the electron stream [see Fig. 1(a)]. Current spikes are clearly visible. The first two spikes

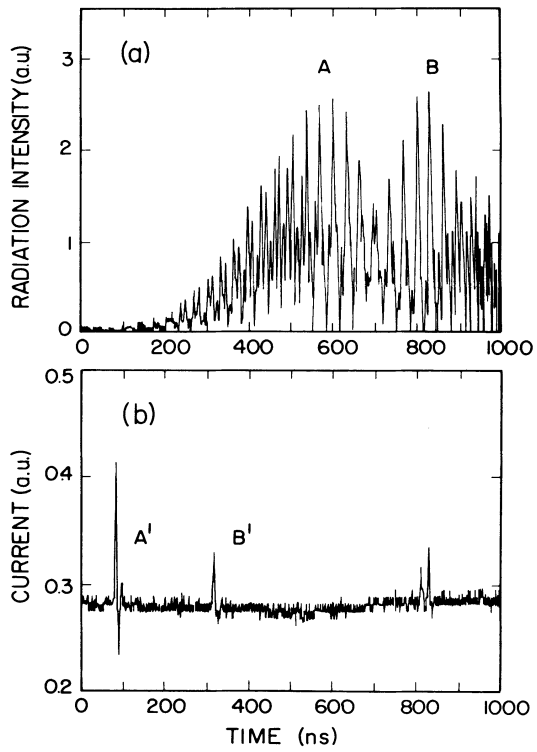

FIG. 2. (a) Expanded oscilloscope traces of partially overlapping radiation bursts, and (b) associated spikes in the electron-beam current density.

marked A' and B' initiate the rf macropulses A and B as will be discussed later. The widths of the current spikes are typically less than 1 ns.

The randomness of the current spike is modeled in the frequency domain within the FEL tuning range as a white noise with a uniform spectral density. Consequently, the electron-beam density at the entrance to the wiggler is described in the time domain as

$$n_i(t) = n_0 + n_n \sum_i \delta(t - t_i) , \tag{1}$$

where n_0 is the dc component of the electron-beam density, n_n is the electron flux associated with the current impulses, and t_i are random points on the time axis. This model of the current spikes is equivalent to the shot-noise model[15–17] applied to a single electron in the beam (the δ function corresponds to single electrons). These current impulses initiate spontaneous FEL emission.

According to basic FEL theory,[18] the response to a current impulse (namely, its temporal Green's function) is a finite pulse of radiation at the FEL resonance frequency. Its pulse width is given by

$$\tau_s = (1/v_z - 1/v_g) L_w , \tag{2}$$

where v_z is the axial electron-beam velocity, v_g is the radiation group velocity, and L_w is the wiggler length. The

time constant τ_s, known as the *FEL slippage time,* is the difference between the propagation times of an electron and a wave packet traveling along the wiggler axis. For our experimental parameters $\tau_s \sim 2.5$ ns. The FEL impulse response is essentially the inverse Fourier transform of the FEL spontaneous-emission spectrum. Hence, $\Delta\omega \sim 1/\tau_s$ is the spectral bandwidth of the FEL spontaneous emission.

The response of the FEL oscillator to a current impulse is more complicated. The immediate response is the short pulse of radiation described above. This pulse, however, is circulating in the ring cavity in successive round-trips. Its frequency corresponds to the FEL resonance, and is amplified by the dc component of the electron-beam current in each round-trip period. This reamplification process continues as long as the FEL resonance conditions are maintained, or until nonlinear saturation takes place.

The FEL oscillator is modeled here as a cascade of FEL blocks[19] as shown in Fig. 3. Each stage l in the cascade represents one round-trip period which consists of an FEL section (FEL$^{(l)}$) and a waveguide section (the delay element D_l). Each FEL block has two inputs; one for the electromagnetic wave E_i, and the other for the electron-beam density fluctuations n_i. Because of the voltage droop in the electron beam, the FEL parameters are slightly time dependent; hence, the FEL blocks have different parameters according to their values in the relevant round-trip period τ_d. Linear transfer functions define the relation between the output $\tilde{E}_o(\omega)$ and the two independent inputs, $\tilde{E}_i(\omega)$ and $\tilde{n}_i(\omega)$, of each block. These are given in the frequency domain for the lth block by

$$\tilde{E}_o(\omega)|_{n_i=0} = T_E^{(l)}(\omega)\tilde{E}_i(\omega)\,, \tag{3a}$$

$$\tilde{E}_o(\omega)|_{E_i=0} = T_n^{(l)}(\omega)\tilde{n}_i(\omega)\,, \tag{3b}$$

where the transfer functions $T_E(\omega)$ and $T_n(\omega)$ are the inverse Laplace transforms of the gain-dispersion equations as derived in the linear theory of the prebunched FEL.[20,21]

The temporal response of the FEL oscillator to a single density impulse is found by an inverse Fourier transform on the cascade transfer function. Assuming that the electron-beam density is given by $n_i(t) = n_0 + n_n\delta(t - t_1)$, the FEL response at $t = t_2$ is given by

$$h_{\rm osc}(t_2,t_1) = \frac{1}{2\pi}\int_\omega T_n^{(0)}(\omega)\prod_{l=1}^{m} T_E^{(l)}(\omega)e^{i\omega t_2 - i\phi_d(\omega)}d\omega\,, \tag{4}$$

where m is the round-trip order corresponding to $t = t_2$, and $\phi_d(\omega)$ is the phase acquired in one round trip in the dispersive waveguide cavity. The FEL response to any electron-density fluctuation $n_i(t) = n_0 + n_f(t)$ is given in general by the convolution integral

$$E_o(t) = \int_{\tau=-\infty}^{t} h_{\rm osc}(t,\tau)n_f(\tau)d\tau\,.$$

In our experiment, we assume that the density fluctuations can be modeled by Eq. (1) and thus the output radiation $E_o(t)$ is related to $h_{\rm osc}(t_2,t_1)$ itself. The validity of this model is limited to rf micropulses shorter than one round-trip time.

The intensity of the impulse response $|h_{\rm osc}(t_2,t_1)|^2$ is computed for the parameters of the FEL used in the experiment, and is shown plotted as a function of time in Fig. 4(a). Figure 4(b) shows the corresponding sweep of the center frequency of each micropulse due to the change in the accelerator voltage shown in Fig. 1(b).

The theoretically calculated impulse-response intensity of the FEL oscillator shown in Fig. 4(a) resembles the

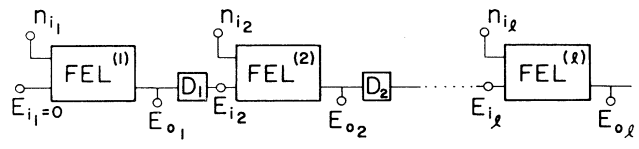

FIG. 3. Schematic of the computational model of the FEL ring oscillator.

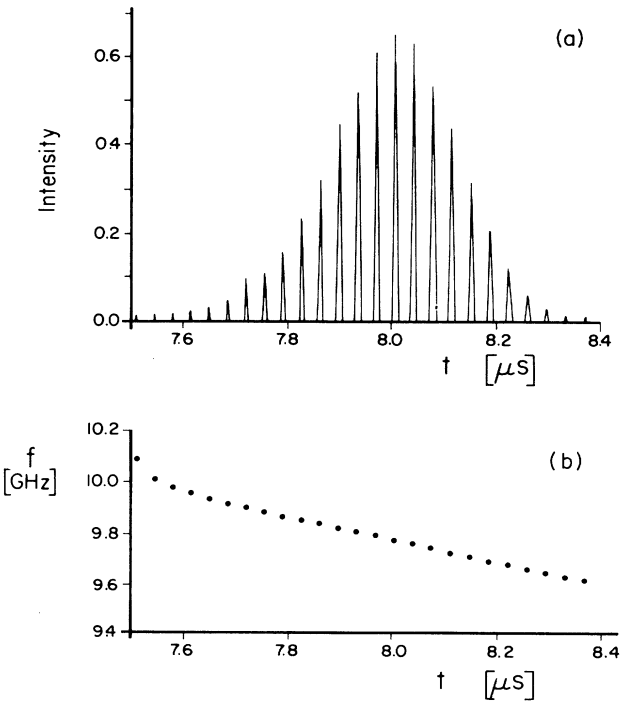

FIG. 4. (a) The computed impulse response of the FEL oscillator [to be compared with the experimental result in Fig. 2(a)], and (b) the corresponding center frequency associated with each successive pulse.

observed bell-shaped macropulses in Fig. 2(a), and the periodic micropulse structure. In the computed FEL impulse response, the macropulse peak point appears 507 ns after the current impulse, the period between two micropulses is 33 ns, and the micropulse width is 5 ns. These theoretical results are quite similar to those in the experimental measurements of Fig. 2(a). The spikes A' and B' appear at $t_{A'}=82$ ns and $t_{B'}=317$ ns, respectively. The peak points of macropulses A and B appear at $t_A=598$ ns and $t_B=827$ ns, respectively. Hence, the time differences $t_A-t_{A'}=516$ ns and $t_B-t_{B'}=510$ ns are nearly the same and agree well with the theoretical result of 507 ns.

It should be noted that the bell-shaped envelope of the macropulse is due to the electron-beam energy droop. This droop leads eventually to a violation of the FEL resonance conditions, and therefore to a reduction in the micropulse growth rate. At the peak of the macropulse, the FEL amplification equals the waveguide attenuation, and the net gain is zero. In the case of a constant electron-beam energy, the reamplification of the micropulse would continue in successive round-trips up to the nonlinear saturation limit.

The micropulse passage in the FEL oscillator is subject to waveguide dispersion and to the FEL phase shift,[22] and therefore its width, as well as its amplitude, is expected to evolve as a function of time. The first micropulse in Fig. 4(a) is the instantaneous response of the FEL to the electron-beam impulse. Its width is the FEL slippage time, $\tau_s \simeq 2.5$ ns. In the following round-trips it slowly broadens to 5 ns near the macropulse peak. This agrees well with the 5.3 ns in the experiment [Fig. 2(a)]. This width equals one-third of the pulse width which would evolve if only waveguide dispersion would occur without the FEL interaction. Hence, both theory and experiment show that the FEL interaction counteracts waveguide dispersion and balances the tendency of the micropulses to broaden.

In conclusion, we have reported what we believe are entirely new observations of an FEL operating near oscillation threshold. The observations show that the radiation field is composed of bursts with a periodic substructure correlated to bursts in the electron-beam current. These studies may contribute to a better understanding of the start-up phase and mode-locking processes in FEL oscillators. They can also shed light on the possible effects of shot noise in FELs that use conventional thermionic or the more recent photocathode guns. Furthermore, our studies may lead to the developments of methods of generating very short, tunable micropulses in free-electron lasers.

This work is supported in part by the National Science Foundation, the Air Force Office of Scientific Research, and the Naval Research Laboratory. E.J. is supported by the Rothschild and Fulbright Foundations.

[a]Permanent address: Faculty of Engineering, Tel Aviv University, Ramet Aviv, 69978, Israel.

[1]P. W. Smith, IEEE J. Quantum Electron. **3**, 627 (1967).

[2]P. W. Smith, Proc. IEEE **58**, 1342 (1970); for recent studies on ultrafast laser phenomena, see the special issue of IEEE J. Quantum Electron. **25** (1989).

[3]L. F. Mollenauer and R. H. Stollen, Opt. Lett. **9**, 13 (1984).

[4]N. M. Kroll and M. N. Rosenbluth, in *Physics and Quantum Electronics* (Addison-Wesley, Reading, MA, 1980), Vol. 7, p. 147.

[5]R. W. Warren, B. E. Newnam, and J. C. Goldstein, IEEE J. Quantum Electron. **21**, 882 (1985).

[6]J. Masud, T. C. Marshall, S. P. Schlesinger, and F. G. Yee, Phys. Rev. Lett. **56**, 1567 (1986).

[7]W. B. Colson, Nucl. Instrum. Methods Phys. Res., Sect. A **250**, 168 (1986).

[8]J. C. Goldstein, B. W. Newnam, R. W. Warren, and R. L. Sheffield, Nucl. Instrum. Methods Phys. Res., Sect. A **250**, 4 (1986).

[9]B. A. Richman, J. M. J. Madey, and E. Szarmes, Phys. Rev. Lett. **63**, 1682 (1989).

[10]J. W. Dodd and T. C. Marshall, in *Proceedings of the Eleventh International Conference on Free Electron Lasers, Naples, Florida,* edited by L. R. Elias and I. Kimel, FEL '89 Conference Digest (IEEE-LEOS, New York, 1989).

[11]T. Kawamura, K. Toyoda, and M. Kawai, Appl. Phys. Lett. **51**, 795 (1987).

[12]E. Jerby, J. S. Wurtele, and G. Bekefi, Bull. Am. Phys. Soc. **35**, 1026 (1990).

[13]J. Fajans, G. Bekefi, Y. Z. Yin, and B. Lax, Phys. Fluids **28**, 1995 (1985).

[14]K. Xu, G. Bekefi, and C. Leibovitch, Phys. Fluids B **1**, 2066 (1989), and references therein.

[15]H. A. Haus, IEEE J. Quantum Electron. **17**, 1427 (1981).

[16]P. Sprangle, C. M. Tang, and I. Bernstein, Phys. Rev. A **28**, 2300 (1983).

[17]K. J. Kim, Phys. Rev. Lett. **57**, 1871 (1986).

[18]C. Brau, *Free Electron Lasers* (Academic, New York, 1990), Chap. 3.

[19]A. Gover, H. Freund, V. L. Granatstein, J. H. McAdoo, and C. M. Tang, *Infrared and Millimeter Waves,* edited by K. J. Button (Academic, New York, 1984), Vol. 11, Chap. 8.

[20]I. Schnitzer and A. Gover, Nucl. Instrum. Methods Phys. Res., Sect. A **237**, 124 (1985).

[21]E. Jerby, Phys. Rev. A **41**, 3804 (1990).

[22]F. Hartemann, K. Xu, and G. Bekefi, IEEE J. Quantum Electron. **24**, 105 (1988).